Supporting Information

1D pair distribution function in the unstretched state

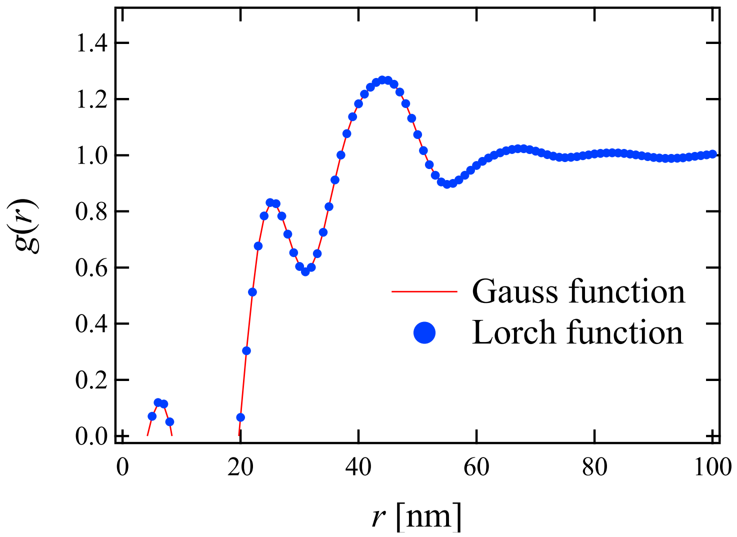

Figure S1: 1D pair distribution function obtained from the circular averaged structure factor by using eq. (S1).

In order to check the validity of eq.(7), we compared 1D slice of 2D PDF to 1D PDF calculated from a circular averaged structure factor in Fig. 4 by using the following equation.

$$g(r) = 1 + \frac{1}{2\pi^2 r n_0} \int_0^\infty dq\, q(S(q) - 1) sin(qr) f(q) \qquad \text{(S1)}$$

Here, n_0 and $f(q)$ are the number density of nano-particles and a window function, respectively. In this study, we checked two types of window functions, i.e., Gauss function and Lorch function.

$$f(q) = exp(-\frac{q^2}{2\sigma^2}) \qquad \text{(S2)}$$

$$f(q) = J_0(\frac{q\Delta}{2}) \qquad \text{(S3)}$$

σ is the standard deviation and we set this value as $\sigma = q_{max}/2$ by following the previous works,[19] where q_{max} is the maximum q value of the measured scattering data. As for Lorch function, we set $\Delta = 2\pi / q_{max}$ by following the previous work.[30] Here, we set $S(q) = 1$ into the circular averaged structure factor from q = 0.6 nm^{-1} to 1.0 nm nm^{-1} and evaluated PDF by using eq. (S1) as shown in Fig. S1. We observed a large positive and negative values in the pair distribution function near r = 0, which seems to derive from the finite q-range for experimental data. The pair distribution function with Gauss function is almost the same as that with Lorch function. In the main text, we will use Gauss function as a window function for circular averaged data. As seen in Fig. S1, we can observe two peaks we observed two peaks at 25 nm and 45 nm. When we take into account the fact that the radius of nanoparticles is ~ 13 nm, the peak at 25 nm indicates that some nanoparticles are in direct contact with each other. The peak at 45 nm correspond to the distances between nanoparticles homogeneously dispersed as discussed in the main text.

Noise reduction

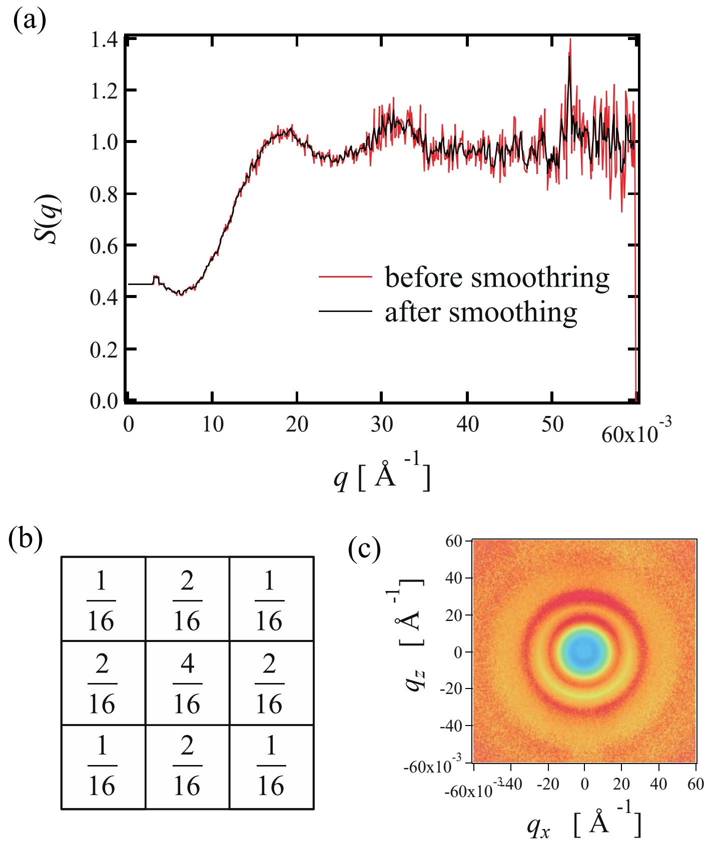

Figure S2. (a)1D plots of structure factor of unstretched PDAM-NP gel before and after smoothing. (b) Schematic illustration for smoothing filter. A center pixel is the pixel of interest. (c) 2D structure factor of unstretched PDAM-NP gel after smoothing.

We checked the effect of noise in scattering profiles, which is frequently discussed in the case of the calculation of 1D PDF from 1D structure factor. In the case of calculation of 2D PDF from 2D structure factor, we observed large noise because we directly divided 2D scattering intensity of nanocomposite gels by that of dilute solution of nanoparticles without taking circular average of 2D scattering patterns. In Fig. S2(a), we plotted 1D slice of 2D structure factor, which is shown in Fig.2. As shown in Fig. S2(a), noise becomes larger and the signal-to-noise ratio decreases in high-q region because signals from samples decreases. In order to remove the noise, we used Gaussian filter. We multiply a constant as shown in Fig. S2(b) to the pixel of interest and surrounding pixels, and put a sum of these pixels into the pixel of interest. The result of smoothing is shown in Fig. S2(a) and (c). We observed the reduction of noise as shown in Fig. S2(a) and (c).

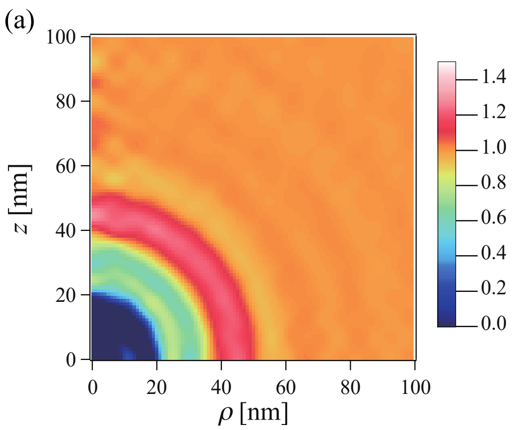

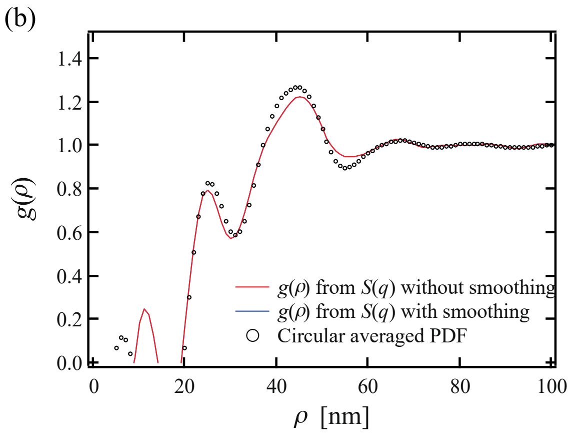

Figure S3. (a)2D PDF evaluated from smoothed structure factor. (b) 1D plot of PDF at $z = 0$.

2D PDF evaluated from smoothed structure factor by using Gauss functions with σ=0.04 Å^{-1} as a window function is displayed in Fig. S3(a). As comparing Fig. 3(b), for which we did not used the smoothed structure factor, to Fig. S3(a), we cannot see a remarkable change before and after smoothing. We plotted PDF at $z = 0$ evaluated from the structure factor with and without smoothing. As shown in Fig. S3(b), PDF evaluated from the structure factor with smoothing is almost identical to that without smoothing. The effect of noise becomes small by summing over random noise in structure factor when we evaluate the PDFs by using eq. (7). In the following, we evaluated PDF without smoothing.

Mask in the vicinity of a beam center

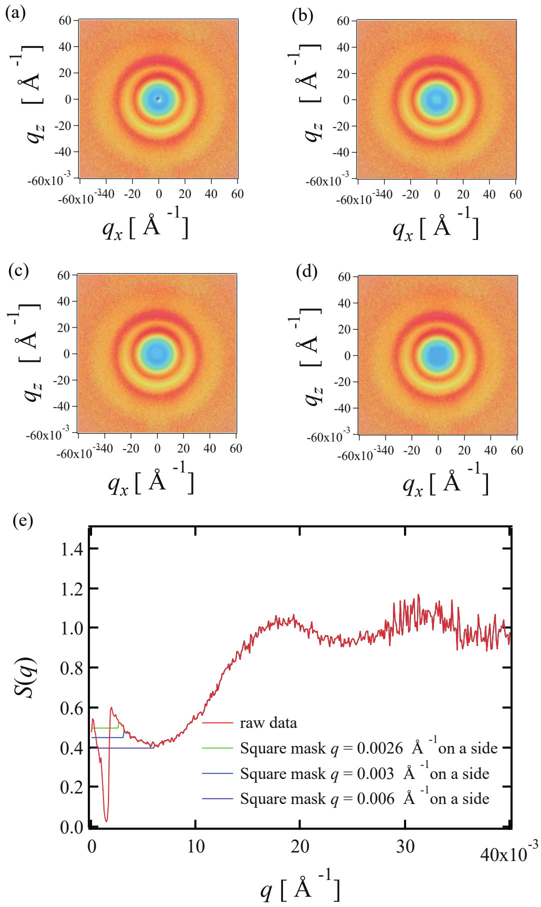

Figure S4. (a) Raw data of the 2D structure factor in the vicinity of a beam stopper. We put square masks with sides (b) q=0.0026 Å^{-1}, (c) q=0.003 Å^{-1} and (d) q=0.006 Å^{-1}. (e) 1D plot of 2D structure factors with several masks.

We plotted the raw data of the 2D structure factors and 1D plots of the 2D structure factors in Fig. S4(a) and (e). As shown in Fig. S4(a) and (e), we observed the upturn in structure factor in the vicinity of a beam center. This upturn may be attributed to parasitic scattering or large aggregates which cannot be evaluated in our experimental set-up. Because this upturn may affect PDF, we applied some masks into 2D structure factor and checked its effect, i.e., we substituted the data by a constant values of 0.5, 0.45, and 0.4 in the range of q=0.0026 Å^{-1}s square, q=0.003 Å^{-1} square, and q=0.006 Å^{-1}s square as shown in Fig. S4(b), (c), and (d), which correspond to the extrapolation of the structure factors to q = 0. Note that Fig. 1(a) is identical to Fig. S4(c). 1D plots of these 2D structure factors were summarized in Fig. S4(e). In order to investigate the effect of these masks, we calculated 2D PDFs from above 2D structure factors. The 2D PDFs calculated from structure factors by using q=0.0026 Å^{-1}s square, q=0.006 Å^{-1}s square, and q=0.003 Å^{-1} square were shown in Fig. S5(a) and (b), Fig. 5(a). As shown in Fig. S5 and 5(a), we cannot observe the effect of masks though q=0.0026 Å^{-1}, q=0.003 Å^{-1}, and q=0.006 Å^{-1} correspond to 240 nm, 200 nm, and 100 nm if we consider Bragg's law d=2π/q, where d is the corresponding spacing. Thus, in the main text, we used q=0.003 Å^{-1}s square mask because we are interested in PDF below 200 nm.

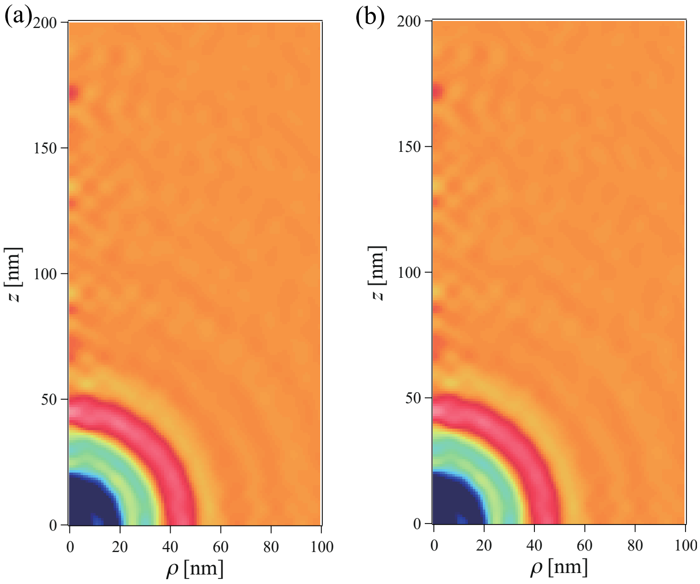

Figure S5. 2D PDFs calculated from 2D structure factors by using square masks with sides (a) q=0.0026 Å^{-1} and (b) q=0.006 Å^{-1}.